

pubs.acs.org/acschemicalbiology Articles

# Time-Dependent Studies of Oxaliplatin and Other Nucleolar Stress-Inducing Pt(II) Derivatives

Hannah C. Pigg, Matthew V. Yglesias, Emily C. Sutton, Christine E. McDevitt, Michael Shaw, and Victoria J. DeRose\*



Cite This: ACS Chem. Biol. 2022, 17, 2262-2271



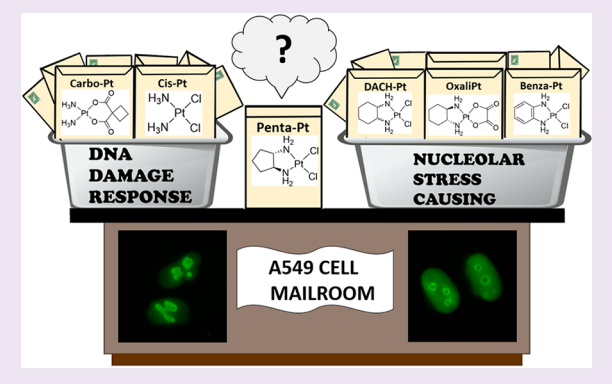
**ACCESS** I

III Metrics & More

Article Recommendations

SI Supporting Information

ABSTRACT: The properties of small molecule Pt(II) compounds that drive specific cellular responses are of interest due to their broad clinical use as chemotherapeutics as well as to provide a better mechanistic understanding of bioinorganic processes. The chemotherapeutic compound cisplatin causes cell death through DNA damage, while oxaliplatin may induce cell death through inhibition of ribosome biogenesis, also referred to as nucleolar stress induction. Previous work has found a subset of oxaliplatin derivatives that cause nucleolar stress at 24 h drug treatment. Here we report that these different Pt(II) derivatives exhibit a range of rates and degrees of global nucleolar stress induction as well as inhibition of rRNA transcription. Potential explanations for these variations include both the ring size and stereochemistry of the non-aquation-labile ligand. We observe that Pt(II) compounds containing a 6-



membered ring show faster onset and a higher overall degree of nucleolar stress than those containing a 5-membered ring, and that compounds having the 1R,2R-stereoisomeric conformation show faster onset and a higher overall degree of stress than those having the 1S,2S-conformation. Pt(II) cellular accumulation and cellular Pt(II)-DNA adduct formation did not correlate with nucleolar stress induction, indicating that the effect is not due to global interactions. Together these results suggest that Pt(II) compounds induce nucleolar stress through a mechanism that likely involves one or a few key intermolecular interactions.

he success of cisplatin as a chemotherapy drug over the last 40 years has led to the investigation of thousands of Pt(II) compounds, only two of which, oxaliplatin and carboplatin, have been approved for clinical use by the FDA. The mechanism of action for Pt(II) compounds has long been attributed to the DNA damage response (DDR).<sup>2</sup> Oxaliplatin, however, exhibits different effects that have been attributed to both the larger diaminocyclohexane (DACH) carrier ligand and the chelating oxalate leaving group (Figure 1, compound 2).3 Recently, it was reported that the cytotoxic effects of oxaliplatin are caused by the ribosome biogenesis stress response instead of the DDR.4 Ribosome biogenesis stress, or nucleolar stress, occurs in the nucleolus and can lead to apoptotic cell death when ribosome biogenesis is disrupted, such as through disruption of the nucleolar structure or through disruption of rRNA synthesis, rRNA processing, or ribosome assembly.<sup>5</sup> Only a few small organic molecules, such as Actinomycin D (ActD), CX-5461, and BMH-21, are known to cause nucleolar stress through RNA Polymerase I inhibition.<sup>6,7</sup> The inclusion of specific mononuclear platinum compounds on this list<sup>4,8-11</sup> would be unique for metallodrugs and also opens new opportunities for mechanistic studies of nucleolar processes.

In previous work, we investigated the structural requirements of platinum compounds necessary to cause nucleolar

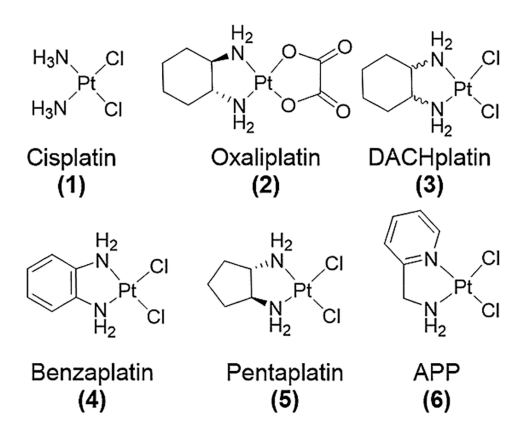


Figure 1. Pt(II) compounds used in this study. DACHplatin is a 1:1 mixture of the 1*R*,2*R* and 1*S*,2*S* isomers. Compounds 2–5 induce nucleolar stress.

Received: May 6, 2022 Accepted: July 20, 2022 Published: August 2, 2022





stress and found at least three derivatives in addition to oxaliplatin that induce robust nucleolar stress responses (Figure 1, compounds 3-5).<sup>8</sup> We found that Pt(II)coordination to the DACH ring, but not the oxalate leaving group, was sufficient to cause the nucleolar stress response as measured by the relocalization of nucleophosmin (NPM1) in mammalian cell culture.<sup>8</sup> Further structure-function analysis found a narrow window of Pt(II) compounds, all containing a cyclic diamino bidentate ligand, that cause nucleolar stress (Figure 1, 3-5).8,11 By contrast, Pt(II) compounds containing alkyl-diamine bidentate ligands do not cause nucleolar stress, even with large substituents.<sup>8</sup> In addition, different orientations of ring substituents such as in picoplatin and 2-aminomethylpyridinedichloride-platinum (APP) (Figure 1, 6) apparently preclude induction of the nucleolar stress response. Stress Phenanthriplatin, a monofunctional Pt(II) compound, also induces robust nucleolar stress but possibly through an alternative mechanism.<sup>4,10</sup> A trinuclear Pt(II) compound has also been shown to affect nucleolar processes.<sup>1</sup> For the oxaliplatin-related Pt(II) compounds investigated here (Figure 1), the sensitivity of the stress response to small ligand changes suggests a model in which the ligand structure of the Pt(II) compound influences a molecular interaction in the nucleolus that induces the nucleolar stress response.

To further probe the mechanism of action of Pt(II) compounds in the nucleolus, we carefully compared effects of cisplatin and oxaliplatin on rRNA transcription and other nucleolar markers. At doses required to induce nucleolar stress, oxaliplatin (but not cisplatin) treatment inhibits rRNA transcription. Further, the onset of rRNA transcription inhibition appears to coincide with or precede NPM1 relocalization as well as changes in other nucleolar markers. Finally, at these treatment conditions, oxaliplatin does not induce DDR markers to the extent that cisplatin does. These results support a model in which cisplatin primarily induces a DDR response, with downstream nucleolar effects, but oxaliplatin induces a primary nucleolar response. Inhibition of rRNA transcription and NPM1 relocalization are likely key factors in the onset of nucleolar stress induction by oxaliplatin.

In our previous work with oxaliplatin-like derivatives,8 nucleolar stress induction by all compounds was measured at 24 h after treatment. At that treatment time, both oxaliplatin and related ring-containing compounds lacking the oxalate leaving group (Figure 1) caused robust nucleolar stress. The relative rates at which these different compounds cause nucleolar stress and their ability to inhibit rRNA transcription are not known. Additionally, the relationships between nucleolar stress induction, cellular platinum accumulation, and DNA binding are not well-established for any platinum compound. In this study we explore the time-dependence of nucleolar stress induction by Pt(II) compounds as measured by NPM1 redistribution. We also measure the extent of rRNA transcription inhibition by these stress-inducing compounds. Additionally, we determine whether cellular platinum accumulation is related to nucleolar stress induction, measured using inductively coupled plasma mass spectrometry (ICP-MS) analysis on whole cell as well as nuclear fractions. We also determine whether in vitro and in cell binding of platinum compounds to DNA correlate with the onset of NPM1 redistribution.

We find that not all stress-inducing Pt(II) compounds induce stress at the same time or even to the same degree. Additionally, we find correlation between rRNA transcription

inhibition and NPM1 redistribution. We also observe that the differences in NPM1 redistribution could not be accounted for by whole cell or nuclear platinum accumulation, or Pt(II)-DNA binding kinetics *in vitro* or in-cell. This indicates that it is not likely the amount of Pt(II) compounds entering cells or the amount binding to DNA that is determining whether a compound will cause nucleolar stress. Finally, we find that the 1R,2R-isomers of pentaplatin and DACHplatin induce a more robust nucleolar stress response when compared to their 1S,2S-isomers. Taken together, these results reinforce the proposal that Pt(II) compounds induce nucleolar stress through a specific molecular interaction and further characterize new Pt(II) compounds that robustly cause inhibition of rRNA transcription.

# ■ RESULTS AND DISCUSSION

Differences in Kinetics of Nucleolar Stress Induction by Pt(II) Compounds. Compounds 2, 3, 4, and 5 (Figure 1) have all been observed to cause nucleolar stress after 24 h of drug treatment time in A549 cells.8 It has previously been observed that oxaliplatin induces slight nucleolar stress as early as 90 min after treatment.9 Structural differences in these stress-inducing Pt(II) derivatives as in DACHplatin (3), with chloride ligands substituting for the chelating oxalate leaving group, an aromatic ring in benzaplatin (4), and a smaller ring size of pentaplatin (5) might influence the rate of inducing nucleolar stress. We used an NPM1 imaging assay<sup>8,10</sup> to determine whether some of these compounds might have a more rapid influence on nucleolar processes than does oxaliplatin. In cells undergoing nucleolar stress, NPM1 is translocated from the granular component (GC) of the nucleolus to the nucleoplasm, 13,14 providing a convenient assay for stress induction. Time points ranging from 30 min to 24 h of drug treatment were tested in A549 cells. A549 cells were chosen because they have wild-type tumor suppressor protein p53, and Pt(II)-induced nucleolar stress has already been characterized in this cell line.<sup>8,9</sup> Each experiment was accompanied by an untreated negative control and positive control of low dose (5 nM) ActD, a known inducer of nucleolar stress via specific inhibition of RNA Polymerase I (Pol I), which transcribes rRNA. 15 Cells were imaged by NPM1 immunofluorescence and the extent of nucleolar stress, based on NPM1 redistribution, was quantified using the calculated coefficient of variation (CV) of NPM1 intensity in each cell.<sup>8</sup> Data were normalized to no-treatment controls. Cells with extensive NPM1 relocalization, indicating nucleolar stress, produce CV values close to that of ActD of around 0.5- $0.7.^{8,1}$ 

Time points of 90 min, 3 h, and 5 h were found to be significant in discriminating the onset of nucleolar stress for the four Pt(II) compounds of interest. Specifically, we saw significant nucleolar stress occurring for DACHplatin by 90 min, oxaliplatin and benzaplatin by 3 h, and pentaplatin by 5 h (Figure 2). ActD as well as cells containing no drug treatment were used as positive and negative controls, respectively.

A comparison of compound structures to the onset of nucleolar stress reveals interesting relationships. Oxaliplatin takes roughly double the time of DACHplatin to induce stress. This is likely due to the slower exchange kinetics of the oxalate leaving group in comparison with the chloride ligands on DACHplatin. However, benzaplatin also takes double the time of DACHplatin to induce stress, indicating that changing the aromaticity of the nonlabile ligand influences the time for

ACS Chemical Biology pubs.acs.org/acschemicalbiology Articles

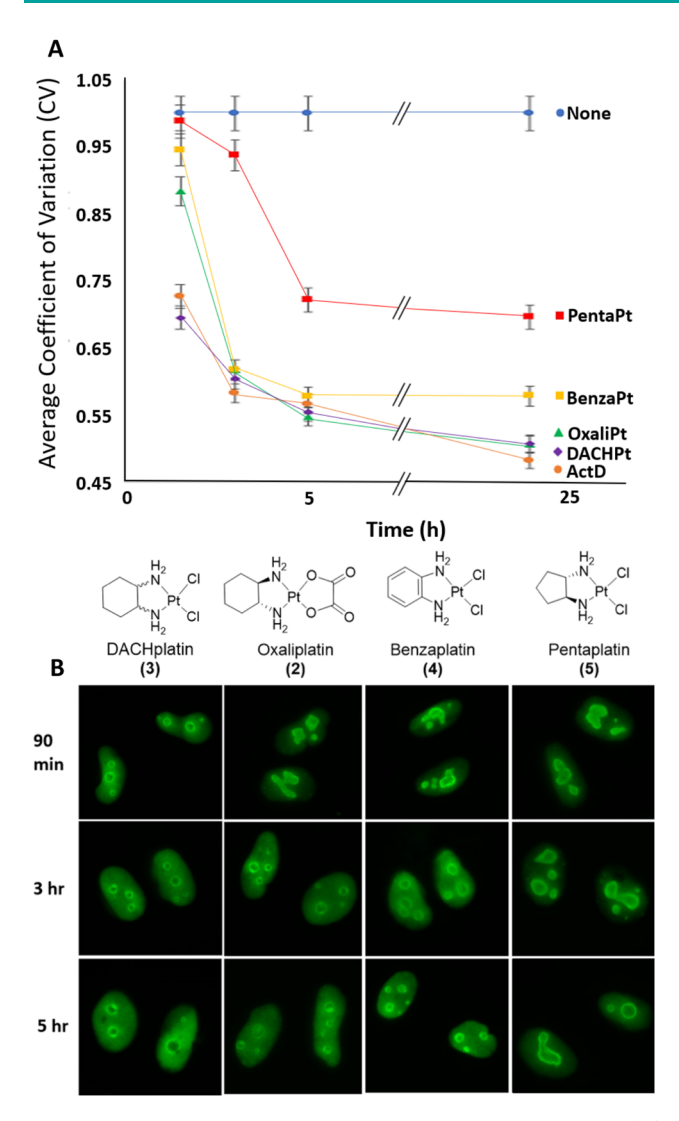


Figure 2. Quantification of NPM1 relocalization induced by Pt(II) compounds at various time points. A549 cells were treated with 10  $\mu$ M of Pt(II) compound or 5 nM ActD and NPM1 distribution was quantified by immunofluorescence (Methods). (A) Each point is the average CV value and standard deviation for 3 biological replicates performed on 3 separate days. (B) Representative cell images of A549 cells treated with each compound at given treatment times.

nucleolar stress induction. As described below, this is not due to slower cellular accumulation of benzaplatin, and therefore may be related to the behavior of the aromatic ring in cells. Finally, the 5-membered ring pentaplatin not only takes longer than the other three compounds to induce detectable NPM1 relocalization, but also shows a lower overall degree of stress, indicated by the higher end point CV of ~0.7. A lower degree of stress induction by pentaplatin was also observed at 24 h in our earlier work. DACHplatin and pentaplatin only vary in the size of the nonlabile ligand ring, indicating that there is likely a specific size that must be met for a compound to induce stress and slightly changing that not only changes the degree of stress that will occur, but also how quickly that compound will induce stress.

Pentaplatin Induces Lower Inhibition of rRNA Transcription. Previous work has shown that oxaliplatin induces nucleolar stress accompanied by early inhibition of rRNA synthesis by Pol I.<sup>9</sup> It was of interest to determine the

relationship between rRNA synthesis inhibition and the range of NPM1 redistribution kinetics observed for compounds 2–5. To measure rRNA transcription, we conducted metabolic radiolabeling experiments using methods previously described. A549 cells were treated with compounds 2–5 for 3 h, and then cells were incubated in drug-free media containing P-labeled phosphate which would be incorporated into any newly synthesized RNA in a pulse step. Media were replaced with cold, drug-containing media for 3 h to track the fate of any radiolabeled RNA. Low dose (5 nM) ActD was used as a positive control for inhibition of rRNA synthesis.

All of the Pt(II) derivatives previously found to induce NPM1 redistribution, compounds 2, 3, 4, and 5, inhibited synthesis of rRNA to an extent similar to the extent of NPM1 redistribution at 3 h (Figure 3). In agreement with previous data,9 a 3 h treatment with oxaliplatin reduced 47S pre-rRNA transcript levels to below 10% of the untreated control, while the fully processed 28S transcript was reduced to roughly 20% of control levels. DACHplatin inhibited rRNA synthesis even more robustly, with both 47S and 28S transcript levels being reduced to under 5% of the untreated control by 3 h. This enhanced inhibition relative to oxaliplatin may be due to more rapid aquation of the labile ligands, greater cellular platinum accumulation, or more extensive disruption of the Pol I transcription machinery. Benzaplatin showed a reduction of both 47S and 28S transcripts comparable to oxaliplatin and consistent with similar levels of NPM1 redistribution at 24 h. While reduction of both rRNA transcripts was observed after pentaplatin treatment, this reduction was modest in comparison to the other platinum compounds and the positive control of ActD. With pentaplatin treatment, 47S transcripts were reduced to about 40% of the negative control, while 28S transcripts were about 50%. This result is consistent with the lower amount of NPM1 redistribution caused by pentaplatin at the 3 h time point (Figure 2).

Next, we wondered if pentaplatin might inhibit rRNA synthesis more robustly after 5 h of drug treatment prior to the pulse step. We also considered whether APP (6), previously shown to not induce nucleolar stress despite structural similarities to the stress-inducing compound benzaplatin,8 could inhibit rRNA synthesis despite its inability to cause NPM1 redistribution. We found that pentaplatin did inhibit synthesis slightly more at 5 h of treatment than at 3 h of treatment, with 47S levels reaching roughly 30% of the negative control, and 28S levels being reduced to 40% (Figure 4). By contrast, APP caused a slight inhibition of rRNA synthesis, although this inhibition was inconsistent and with a high standard deviation over three trials with separate biological replicates. With APP treatment, 47S and 28S levels were reduced to around 85% and 50% of the untreated control levels respectively (Figure 4).

Similar levels of rRNA synthesis inhibition are incurred by cisplatin treatment at 3 h, which we previously attributed to effects downstream of the DDR. In conclusion, all Pt(II) derivatives that induce NPM1 relocalization by 24 h also induce significant inhibition of rRNA synthesis by 3 h of treatment, with DACHplatin causing the most robust inhibition and pentaplatin inducing only modest inhibition. Pentaplatin inhibition of rRNA synthesis intensifies by 5 h of treatment, consistent with the further extent of NPM1 redistribution.

Whole Cell and Nuclear Platinum Accumulation Do Not Correlate with Nucleolar Stress Induction by Pt(II)

ACS Chemical Biology pubs.acs.org/acschemicalbiology Articles

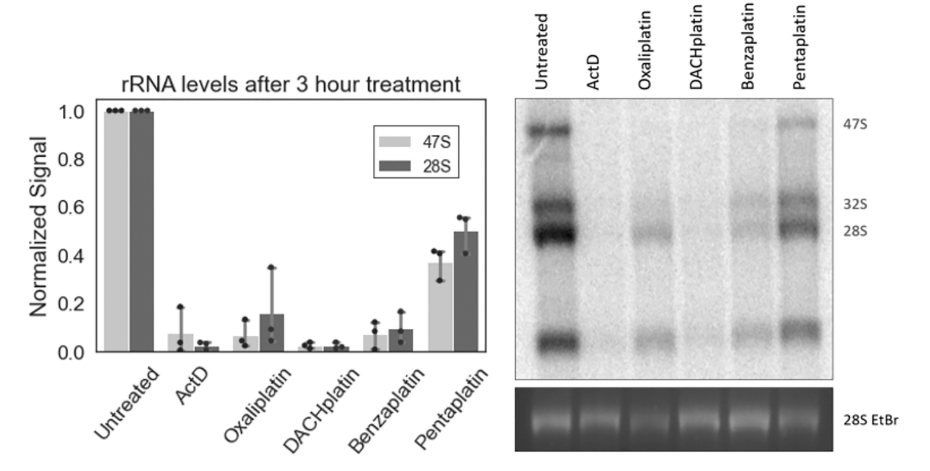
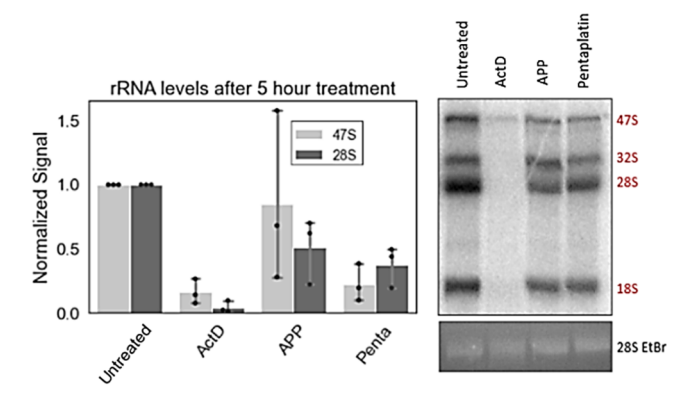


Figure 3. Metabolic labeling to measure rRNA synthesis and processing at 3 h of treatment. Cells were treated with  $10 \mu M$  platinum compounds or 5 nM of ActD for 3 h prior to a 1 h pulse step, followed by a 3 h chase step. Bottom frame in the gel image shows total RNA (EtBr stain of 28S rRNA) while the top image shows  $^{32}$ P-labeled rRNA. Transcript sizes are shown on the right. Error bars represent the standard deviation of three replicates of A549 cells across three separate days.



**Figure 4.** Metabolic labeling to measure rRNA synthesis and processing at 5 h of treatment. Cells were treated with  $10~\mu M$  platinum compounds or 5 nM of ActD for 5 h prior to the pulse step. Bottom frame in gel image shows total RNA (EtBr stain of 28S rRNA) while top image shows  $^{32}$ P-labeled rRNA. Transcript sizes are shown on the right. Error bars represent the standard deviation of three replicates of A549 cells across three separate days.

Compounds. Pt(II) compounds can enter the cell either through passive diffusion or active transport and their uptake is highly dependent on the size, charge, and lipophilicity of the complex. While it is generally believed that passive diffusion is the primary way by which Pt(II) compounds enter the cell, certain transport proteins, such as the organic cation transporter and the copper transporter 1 (CTR1), are also known to facilitate Pt(II) uptake. We questioned whether cellular uptake and accumulation influenced the rates of nucleolar stress induction observed for different Pt(II) compounds. To quantify the cellular accumulation of compounds 1–5, we utilized ICP-MS to determine the platinum content in whole cell lysate, nuclear fractions, and DNA extracted from treated A549 cells. 20–22

Average cellular platinum accumulation at 90 min, 3 h, and 24 h after treatment with  $10~\mu M$  of each Pt(II) compound are summarized in Figure 5A. Cellular accumulation for each Pt(II) compound was quantified by the amount of platinum measured by ICP-MS relative to the total protein mass in each sample (ng Pt/mg protein). The measured cellular platinum accumulation over time for each of the stress-inducing Pt(II) compounds (Figure 5A) follows a general trend that does not

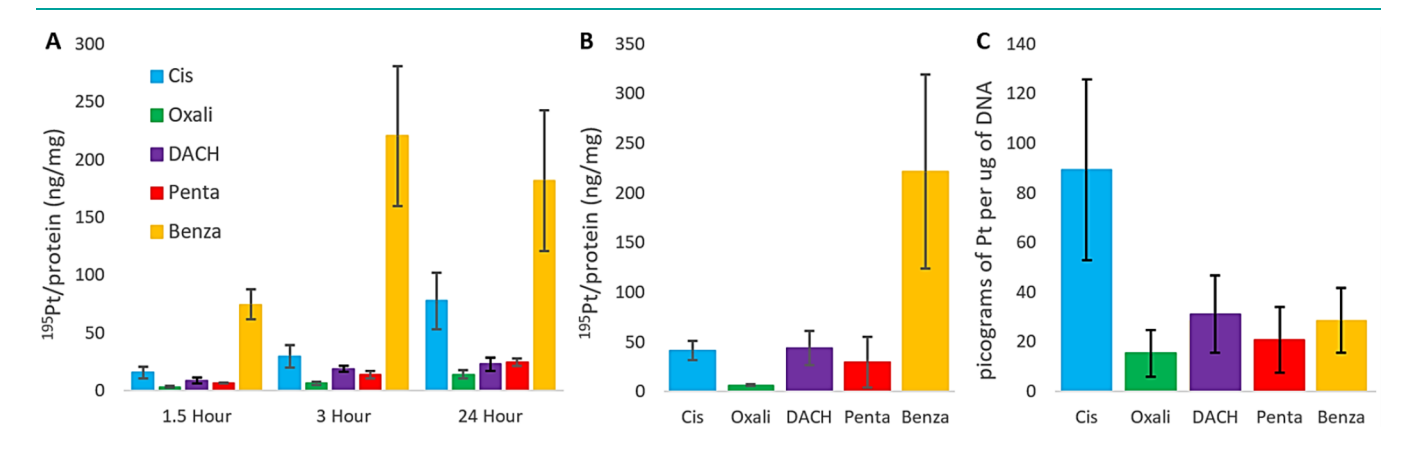


Figure 5. Platinum content in whole cell, nuclear, and DNA samples measured by ICP-MS. (A) Cellular platinum content at varying drug treatment times. (B) Platinum in nuclear fractions at 24 h drug treatment time. (C) Platinum content in DNA extracted from cells at 24 h drug treatment time. (A) and (B) are averages of 3 biological replicates. Measurements in (C) reflect 5 biological replicates. All measurements are from A549 cells treated with  $10 \mu M$  platinum compound.

correlate to the time points where nucleolar stress is observed. Cellular accumulation of cisplatin was observed to be significantly higher than oxaliplatin and DACHplatin, which agrees with previous studies. Cellular accumulation for oxaliplatin was observed to be lower than the nonoxalate derivative, DACHplatin, which is likely due to the slower aquation rate of oxaliplatin compared to DACHplatin. Surprisingly, we found that the measured platinum accumulation in cells treated with 10  $\mu$ M of benzaplatin was significantly higher than the other Pt(II) compounds tested, at all time points. The higher cellular accumulation of benzaplatin may be due to hydrophobicity, or to the observation that Pt(II) complexes with aromatic diamine ligands, such as benzaplatin, have been shown to undergo rapid exchange of labile Cl<sup>-</sup> ligands.

In addition to whole cell platinum accumulation studies, we also measured platinum levels in nuclear extracts of cells treated with compounds 1–5 for 24 h (Figure 5B). The results from these studies closely mimicked those seen for whole cell platinum accumulation. Benzaplatin again showed the highest levels of nuclear accumulation, whereas oxaliplatin showed the lowest levels of nuclear accumulation. Additionally, there does not appear to be any correlation between the onset of nucleolar stress and nuclear platinum accumulation. This suggests that nuclear platinum accumulation is also less sensitive to the minor structural changes that modulate the nucleolar stress response.

Pt(II)-DNA Binding *In Vitro* and in Cell Does Not Correlate with Nucleolar Stress Induction. It is widely accepted that the cytotoxicity of platinum compounds is at least in part due to the formation of DNA-platinum adducts, <sup>24</sup> which are primarily 1,2-intrastrand cross-links on adjacent guanines. <sup>25,26</sup> Because of this, the understanding of binding kinetics and adduct formation of oxaliplatin and cisplatin to DNA has been a topic of interest for many decades. <sup>27–29</sup> Pt(II)-DNA adducts form more rapidly following cisplatin treatment than oxaliplatin treatment, and to a higher extent following cisplatin treatment both *in vitro* with varying DNA types and in multiple cell lines. <sup>30</sup> Although the DNA binding characteristics of cisplatin and oxaliplatin have been extensively covered in the literature, little is known about the relationship between DNA platination and nucleolar stress induction.

To further investigate the relationship between DNA platination and nucleolar stress induction, we measured relative DNA-platinum adduct amounts for compounds 1-5 in a model oligonucleotide and in DNA extracted from treated A549 cells. Model oligonucleotide studies measured platinum binding to a short DNA hairpin sequence containing adjacent guanines (TATGGTATTTTTATACCATA) analyzed by dPAGE following incubation times from 90 min to 24 h (Figure S1). By 24 h, all compounds except oxaliplatin and benzaplatin appear to bind in similar amounts showing ~100% relative intensity of platinated to non-platinated DNA. Based on previous work, in these model studies oxaliplatin was expected to show slower overall binding and less adduct formation than cisplatin, but it is notable that at 3 h treatment, oxaliplatin treatment induces significant nucleolar stress in cells. Another interesting result obtained from this study was that benzaplatin appeared to show no binding to the hairpin DNA at 24 h incubation, even though it shows stress induction in cells (Figure S1). The reason for this observation is not known, but it is possible that due to the aromatic ring,

benzaplatin may be forming a species in solution that is preventing interaction with the hairpin DNA.

To further investigate the relationship between Pt(II)-DNA adduct formation and nucleolar stress induction, we quantified the amount of Pt(II)-DNA adduct in A549 cells that formed after 24 h of incubation with compounds 2-5 (Figure 5C) using ICP-MS. The results from the in-cell Pt(II)-DNA binding assays showed some notable differences compared to the in vitro studies. As expected, cisplatin showed significantly more binding to cellular DNA at 24 h than oxaliplatin.<sup>31</sup> Unlike in the model studies, where cisplatin seemed to bind at similar rates as both DACHplatin and pentaplatin, the in-cell binding assays indicated that cisplatin binds to DNA in a higher amount than any of the stress-causing compounds. Importantly, pentaplatin, which shows less overall nucleolar stress at 24 h compared to the other oxaliplatin-like compounds of interest, shows relatively the same amount of in-cell DNA binding as DACHplatin and benzaplatin, indicating that it is not likely the ability of pentaplatin to bind to DNA that is causing it to show less nucleolar stress. Finally, benzaplatin, which did not exhibit any DNA binding in the in vitro studies, has in-cell Pt(II)-DNA levels that are similar to those of the other nucleolar stress-causing compounds. This indicates that there may be some cellular interaction occurring with benzaplatin that is allowing it to bind to DNA that is not occurring in buffered solution. Understanding this reaction may help to better understand the nucleolar stress pathway and how it differs from DDR induced by cisplatin and carboplatin. Based on these results, it can be concluded that whether a compound will cause nucleolar stress is not likely directly related to the rate of DNA platination or the overall level of Pt(II)-DNA adduct formation.

Chirality of Pt(II) Compounds Influences the Degree of Nucleolar Stress. It has previously been reported that the 1R,2R- and 1S,2S-isomers of DACHplatin and pentaplatin have different DNA-binding properties, with the 1S,2S-isomer of both compounds showing more interstrand DNA crosslinking compared to the 1R,2R-isomer. 32,28 Growth inhibition studies in the NCI-60 human tumor cell lines panel show that the 1R,2R-isomer of DACHplatin is nearly 5 times more potent when compared to the 1S,2S-isomer.<sup>33</sup> In a study of acridine-linked monofunctional Pt(II) compounds, the 1R,R-DACHplatin isomer was also slightly more toxic when measured in A549 cells.<sup>34</sup> The previous experiments in our study used a racemic mixture for DACHplatin, but only the 1S,2S-isomer for pentaplatin.8 We questioned whether the 1S,2S-isomer of pentaplatin was the source of lower levels of nucleolar stress induction observed for this compound. To test this, we performed NPM1 relocalization studies with pure 1S,2S- and 1R,2R-isomers of both pentaplatin and DACHplatin (7-10, Figure 6).

We find that there is indeed a relationship between a Pt(II) compound's isomeric form and its ability to induce nucleolar stress. The 1R,2R-isomer of pentaplatin induces nucleolar stress at an earlier time point and to an overall higher degree than does the 1S,2S-isomer (Figure 7). Specifically, at the 3 h time point the pentaplatin 1R,2R-isomer is causing robust nucleolar stress (CV = 0.65), while the pentaplatin 1S,2S-isomer is not (CV = 0.88). While both compounds are inducing nucleolar stress at longer treatment times, the pentaplatin 1R,2R-isomer is causing a higher degree of stress than the pentaplatin 1S,2S-isomer at both 5 and 24 h time points.

**Figure 6.** Pt(II) compounds used in isomer-specific NPM1 relocalization studies.

We next measured NPM1 relocalization following treatment with either the 1R,2R- or 1S,2S-isomer of DACHplatin. We find the same trends as observed for the two isomers of pentaplatin, however not to the same degree (Figure 8). At the 90 min time point, the DACHplatin 1R,2R-isomer induces significant nucleolar stress (CV = 0.73) while the DACHplatin  $1S_{2}S$ -isomer (CV = 0.96) does not exhibit much of an effect on NPM1 relocalization. Additionally, at the 3 h time point, the DACHplatin 1R,2R-isomer shows a higher degree of stress (CV = 0.67) than the DACHplatin 1S,2S-isomer (CV = 0.80). By 24 h, however, both isomers of DACHplatin show relatively the same degree of nucleolar stress; this differs from the case of pentaplatin, where the pentaplatin 1S,2S-isomer (CV = 0.68) does not reach the same degree of nucleolar stress as the pentaplatin 1R,2R-isomer (CV = 0.53) by 24 h. These comparisons indicate that although the stereochemistry plays a role in the degree of nucleolar stress induced by these compounds, the size of the ring is still involved and the 6membered DACH ring is more effective at inducing nucleolar stress than is the 5-membered ring of pentaplatin.

Based on these data it appears that some property of the 1S,2S-isomers, and specifically the pentaplatin 1S,2S-isomer, makes it less ideal for NPM1 relocalization and nucleolar stress induction. It has previously been suggested that the bend and

unwinding angles of the DNA double helix caused by platinum cross-linking are slightly different for the two isomers and that the amino protons of the 1S,2S-isomer have different hydrogen bonding interactions than in the 1R,2R-isomer when bound to DNA. Energy-minimized structures of 1R,2R- and 1S,2S-pentaplatin are shown in Figure 9. When bound to DNA or RNA, the 1R,2R- and 1S,2S-isomers would present slightly different faces in the 3'- and 5'-directions that could influence nucleic acid structure or interactions with binding partners or polymerases. To visualize these potential differences, the structures are oriented "end-on" to show relative orientations of -NH<sub>2</sub> groups as well as orientation of steric bulk. Stereospecific interactions are also possible when bound to nucleolar proteins.

# CONCLUSIONS

It has long been known that oxaliplatin and cisplatin induce different cellular effects and vary in the cancers that the compounds are most effective in treating. Some variations between these compounds include differences in their ability to form cellular Pt(II)-DNA adducts, variations in their cytotoxicity across various cell lines, and differences in the chemotherapeutic side effects induced by these compounds in cancer patients. 30,36,37 Although there is much research surrounding both cisplatin and oxaliplatin, the cellular mechanisms that induce the variations between these two compounds are not well understood. It has been reported that unlike cisplatin, oxaliplatin does not induce cell death via DDR, but rather through ribosome biogenesis stress, or nucleolar stress.<sup>4</sup> Our lab has previously tested a limited library of Pt(II) compounds and found a subset that cause nucleolar stress induction.<sup>8,10,11</sup> Here we performed more thorough investigations with four-stress inducing Pt(II) compounds we had previously identified: oxaliplatin, benzaplatin, DACHplatin, and pentaplatin (2-5).

We were first interested in determining relative rates of nucleolar stress induction based on NPM1 relocalization from the nucleolus to the nucleoplasm. We found that not all stress inducing Pt(II) compounds induce nucleolar stress at the same time or even to the same degree (Figure 2). Further, there are measurable differences in the levels of nucleolar stress induced by 1*R*,2*R*- and 1*S*,2*S*-isomers (Figures 7,8). Specifically, we see

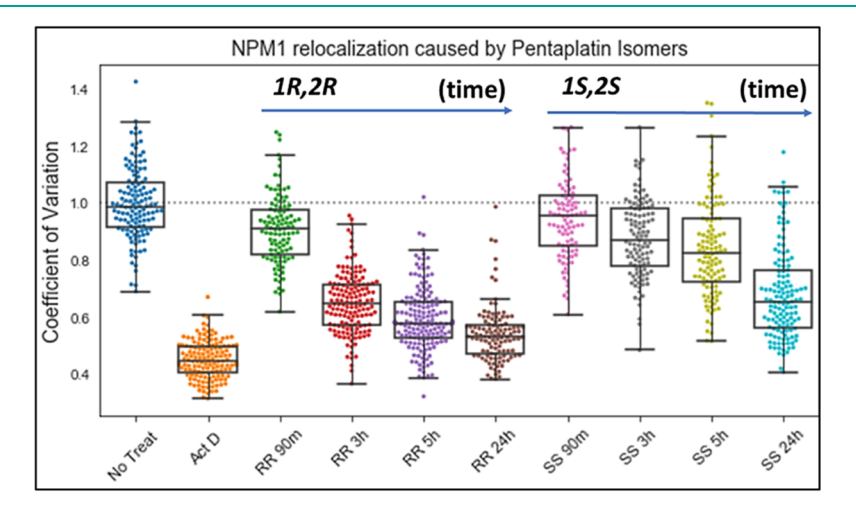


Figure 7. Quantification of NPM1 relocalization induced by pentaplatin isomers. Treatment conditions are the same as in Figure 2. For each treatment individual dots represent single cells, data set boxes represent median, first, and third quartiles, and vertical lines are the range of data.

ACS Chemical Biology pubs.acs.org/acschemicalbiology Articles

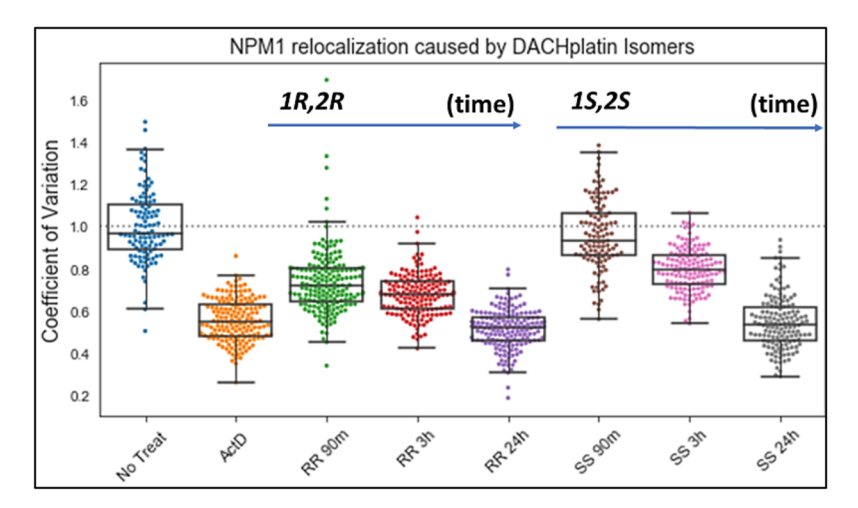
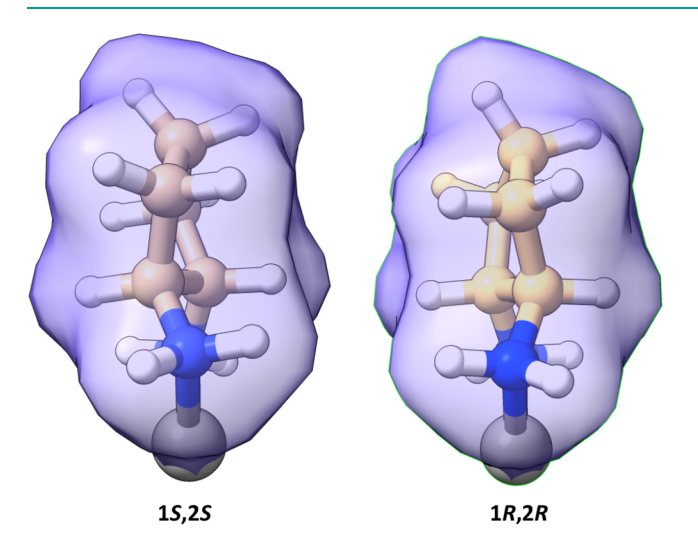


Figure 8. Quantification of NPM1 relocalization induced by DACHplatin isomers. Treatment conditions are the same as in Figure 2. For each treatment individual dots represent single cells, data set boxes represent median, first, and third quartiles, and vertical lines are the range of data.



**Figure 9.** Lowest-energy conformations of pentaplatin in the 1*S*,2*S*-and 1*R*,2*R*-configurations (see Methods). Chloride ligands have been removed.

that 1R,2R-DACHplatin causes nucleolar stress earlier than the other stress inducing compounds, initially observed at 90 min. By contrast, 1S,2S-pentaplatin does not induce stress until a longer time point of 5 h and to a lesser overall degree. This indicates that there are likely some intermolecular interactions occurring with the Pt(II) stress-inducing compounds that allow certain enantiomers to be favored over others in terms of inducing stress.

Next, we sought to confirm that stress causing compounds cause an inhibition of rRNA transcription as previously observed for oxaliplatin. From these studies (Figures 3,4) there appears to be a direct correlation between rRNA transcription inhibition and observation of nucleolar stress by NPM1 redistribution. This correlation is particularly apparent when observing 1S,2S-pentaplatin, which showed less NPM1 redistribution than the other stress causing compounds and also showed less rRNA transcription inhibition. 1S,2S-pentaplatin still exhibits rRNA transcription inhibition in comparison with untreated cells, but not to the same degree as oxaliplatin, DACHplatin, and benzaplatin, suggesting that ring

size has a significant influence on the ability to cause nucleolar stress in this class of Pt(II) compounds.

We were then interested in determining if cellular accumulation of Pt(II) compounds or DNA binding could account for the differences in nucleolar stress induction (Figure 5). From ICP-MS cellular platinum accumulation studies, we found that there does not appear to be a correlation between a compound's ability to enter and remain in cells and its ability to cause nucleolar stress. 1S,2S-pentaplatin showed similar whole cell and nuclear platinum accumulation to that of oxaliplatin and DACHplatin even though it was causing less overall nucleolar stress then these compounds. Interestingly, benzaplatin exhibits much higher cellular accumulation than all other Pt(II) compounds tested. The specific reason for this is still not well understood but is potentially related to the aromaticity of the benzene ring and its ability to form reactive species that may allow it to be taken up by cells more easily.

Finally, we looked at the rate and overall amount of Pt(II)-DNA adducts being formed both in vitro and in-cell for both stress inducing and nonstress inducing Pt(II) compounds. While cisplatin bound to a DNA hairpin at a similar rate in vitro as the other stress-inducing compounds, it is bound at a much higher relative level in DNA extracted from cells treated for 24 h. This indicates that induction of nucleolar stress does not require higher levels of binding to cellular DNA than for compounds that cause cell death via DDR. Additionally, there appeared to be low correlation between the degree of stress a compound caused, and the level of DNA adducts formed. This can be observed when comparing oxaliplatin, which showed a lower amount of DNA adduct formation and a higher degree of nucleolar stress, to 1S,2S-pentaplatin, which showed a higher amount of adduct formation and a lower degree of nucleolar stress. Although DACHplatin and pentaplatin were found to differ significantly in their onset and degree of nucleolar stress (Figure 2), the platinum content in cells, nuclear extracts, and extracted DNA from treated cells are remarkably similar (Figure 5). These results indicate that cellular platinum accumulation is less sensitive to the minor structural changes that modulate the nucleolar stress response.

Overall, the sensitivity of nucleolar stress induction to size and stereochemistry of cyclic diamine Pt(II) ligands points toward a model by which oxaliplatin-related Pt(II) compounds induce nucleolar stress via a mode that is highly specific and

likely involves one or a few key intermolecular interactions. These interactions result in early inhibition of rRNA transcription and disruption of nucleolar structure. Future studies will focus on continuing to understand the Pt(II)-induced nucleolar stress pathway and identifying key molecular interactions that occur or are inhibited in order to cause Pt(II)-induced nucleolar stress.

# METHODS

**Cell Culture and Treatment.** A549 human lung carcinoma cells (#CCL-185, American Type Culture Collection) were cultured at 37 °C, 5% CO<sub>2</sub> in Dulbecco's Modified Eagle Medium (DMEM) supplemented with 10% Fetal Bovine Serum (FBS) and 1% antibiotic—antimycotic. Treatments were conducted on cells that had been grown for 11–30 passages to 70–80% confluency. Platinum compound treatments were conducted at 10 μM and Actinomycin D treatments were conducted at 5 nM unless otherwise noted. Actinomycin stocks were stored frozen in DMSO and thawed on day of use. Platinum compounds were made into 5 mM stocks on the day of treatment from solids in 0.9% NaCl (cisplatin), water (oxaliplatin), or DMF (remaining platinum compounds). Stock solutions were diluted into media immediately prior to drug treatment.

Time-Dependent NPM1 Redistribution. Immunofluorescence. Cells were grown on coverslips (Ted Pella product no 260368, Round glass coverslips, 10 mm diam, 0.16-0.19 mm thick) according to the methods previously described.<sup>8</sup> After platinum drug treatment, cells were washed 2× with phosphate buffered saline (PBS) and fixed with 4% paraformaldehyde in water at RT. Paraformaldehyde was then removed, and cells were permeabilized using 0.5% Triton-X in PBS for 20 min at RT. Cells were then washed with 1% bovine serum albumin (BSA) in PBST (PBS with 0.1% Tween-20) for 10 min 2x. Following this, cells were incubated with the primary antibody (NPM1 Monoclonal Antibody, FC-61991, from Thermo-Fisher, 1:200 dilution in PBST with 1% BSA) for 1 h. Cells were then washed with PBST for 5 min 3× and then incubated with secondary antibody (Goat Anti-Mouse IgG H&L Alexa Fluor 488, ab150113, Abcam, 1:1000 dilution in PBST with 1% BSA) for 1 h. Cells were then washed again with PBST for 5 min 3× before mounting. Coverslips were mounted on slides with ProLong Diamond Antifade Mountant with DAPI (Thermo Fisher) according to manufacturer's instructions.

Image Processing and Quantification. Images were taken using a HC PL Fluotar 63×/1.3 oil objective mounted on a Leica DMi8 fluorescence microscope with Leica Application Suite X software. Quantification of NPM1 relocalization was performed in an automated fashion using a Python 3 script.8 Images were preprocessed in ImageJ<sup>38</sup> to convert the DAPI and NPM1 channels into separate 16-bit grayscale images. Between 70 and 225 cells were analyzed for each treatment group. Nuclei segmentation was determined with the DAPI images using Li thresholding functions in the Scikit Image Python package.<sup>39</sup> The coefficient of variation (CV) for individual nuclei, defined as the standard deviation in pixel intensity divided by the mean pixel intensity, was calculated from the NPM1 images using the SciPy Python package. All data were normalized to the notreatment control in each experiment. NPM1 imaging results for each compound were observed on a minimum of three separate testing days.

rRNA Transcription Inhibition. A549 cells were grown to 70% confluency in a 6-well tissue culture plate. Drug treatment was completed for three or 5 h prior to the pulse step with the compounds indicated in DMEM supplemented with 10% FBS and 1× antibiotic—antimycotic. One hour prior to the pulse step, phosphate depletion was performed by switching regular media for phosphate-free media with 10% FBS, 1× antibiotic—antimycotic, and the drug of interest. For the pulse step, media was replaced with a solution of 15  $\mu$ Ci/ml <sup>32</sup>P orthophosphate made in phosphate-free media with FBS and antibiotic—antimycotic. After the 1 h pulse step, media was replaced with cold drug-containing DMEM with FBS and antibiotic—

antimycotic for a 3 h chase. RNA was then extracted using the Zymo Quick-RNA Miniprep kit and separated by size on an agarose gel. The gel was then visualized in two ways: Total RNA was (1) visualized with an ethidium bromide stain and (2) radioactively labeled RNA produced during the pulse step was visualized. To visualize radiolabeled RNA, the gel was dried on Whatman paper using a gel dryer set for 2 h at 70 °C, after which it was left on the gel dryer overnight at RT. The dried gel was exposed to a phosphor screen for 24 h, and the screen was imaged using a Storm phosphorimager. The amount of labeled RNA was quantified by calculating the intensity of the gel bands in the images in ImageJ.<sup>3</sup> Prior to quantification, gel files from the Storm software were converted from square root encoding to linear encoding using the Linearize GelData ImageJ plugin.<sup>38</sup> Quantified radiolabeled RNA was normalized to the total 28S RNA levels for each sample, measured by EtBr. The band marked 47S includes the 47S primary transcript and 45S early pre-rRNA processing intermediate. 17 RNA transcript amounts are shown on graphs as a fraction of the mean untreated control intensities for each experiment.

**Cellular Platinum Accumulation.** *Cell Treatment and Sample* Preparation. A549 cells were seeded in a 10 cm culture dish and incubated for at least 24 h or until at least 80% confluent, prior to treatment. Cell treatments were performed following the general treatment protocol. After incubation, the treatment media were aspirated, and cells were thoroughly washed three times with warm PBS (2 mL). Cells were harvested by trypsinization using 1 mL of TrypLE Express Enzyme (Thermo Fisher) and collected in 4 mL of DMEM in a 15 mL falcon tube. The cell suspension was then centrifuged (2000 rpm, 7 m), and the cell pellets were resuspended in 2 mL of cold PBS. The cell suspension was then transferred into two 1.5 mL Eppendorf tubes in separate 1 mL aliquots for acid digestion and protein concentration quantification, respectively. The samples were then centrifuged (3000 rcf, 10 m, 4  $^{\circ}\text{C})$  and the supernatant was carefully aspirated. Cell pellets for protein quantification were resuspended in 500 µL of ice-cold RIPA buffer containing mammalian protease inhibitor cocktail (Sigma-Aldrich). Samples for acid digestion and protein quantification were stored at -20 °C.

Determination of Total Protein Concentration. Cell suspension for total protein analysis were lysed by vortexing on high for 15 min in 5 min increments. Total protein concentration was assayed by BCA (bicinchoninic acid) assay using a Pierce BCA Protein Assay Kit (Thermo Fisher) following the manufacturer's protocol (96-well plate). Optical density was measured on a microplate reader (Tecan Spark 20M).

Cell Fractionation. For subcellular platinum quantification, after treatment, the media were aspirated, and cells were thoroughly washed three times with warm PBS (2 mL). Cells were harvested by trypsinization using 1 mL of TrypLE Express Enzyme (Thermo Fisher) and collected in 1 mL Tris-KCl buffer (100 mM KCl, 50 mM Tris HCl, pH 7.5, 5 mM MgCl<sub>2</sub>, 1 mM Na<sub>2</sub>EDTA), a 200 µL aliquot was taken for whole cell platinum accumulation analysis. The remaining sample was centrifuged (2 m, 1000g, 4 °C), and the supernatant was aspirated. Cell pellets were resuspended in 100  $\mu L$  of cold lysis buffer and set on ice for 15 min followed by addition of 700  $\mu$ L Tris-KCl buffer. Lysate was centrifuged (10 m, 12000g, 4 °C), and a 500  $\mu$ L aliquot of the supernatant (cytoplasmic fraction) was collected and stored at −20 °C until digestion. Crude nuclei pellet was resuspended in 1 mL Tris-KCl buffer and centrifuged (10 m, 12000g, 4 °C). Supernatant was aspirated and purified pellets were stored in 200  $\mu$ L lysis buffer at -20 °C until digestion.

Acid Digestion. Cell pellets for acid digestion were first heated on a heat block at 65–70 °C in open air until completely dry. Then, 100  $\mu$ L of concentrated nitric acid (69%, TraceSELECT, Fluka) was then added to each dry cell pellet, and the sealed samples were heated at 65–70 °C on a heat block overnight. Digested samples were then cooled to RT and diluted with 900  $\mu$ L of dH<sub>2</sub>O to a final volume of 1 mL.

*ICP-MS Total Platinum Concentration Analysis.* Platinum concentrations were determined by ICP-MS (Thermo Scientific, iCAP RQ ICP-MS) equipped with a CETAC ASX-500 autosampler.

The instrument was tuned daily with an ICP-MS tuning solution (Tune B iCAP Thermo TS, Inorganic Ventures) for optimal conditions. All CPS measurement were made in kinetic energy discrimination (KED) mode. Measured platinum concentrations for each trial represent the average of three scans. Calibration standards were prepared from a platinum standard solution (1001  $\pm$  5  $\mu g/mL$ , Inorganic Ventures). Bismuth, indium, terbium, and yttrium from a multielement internal standard solution (10  $\mu g/mL$ , Inorganic Ventures) were used as internal standards (1 ppb) to monitor instrument drift and matrix effects. 2% (v/v) HNO $_3$  (TraceSELECT, Fluka) was used for dilution of standards and digested samples. Calibration standards were prepared fresh each day from the platinum standard solution to a concentration of 0.50, 1.00, 2.00, 4.00, 10.00, 20.00, 40.00, 100.00, and 200.00 ppb. Prepared digested samples diluted by a factor of 1:4 prior to measurement to a total volume of 4 mL.

Model Oligonucleotide DNA-Pt(II) Adduct Assays. Hairpin DNA sequence (TATGGTATTTTTATACCATA) (280  $\mu$ M) was folded by rapid heating to 90 °C and slow cooling to 4 °C in 10 mM Na<sub>2</sub>HPO<sub>4</sub>/NaH<sub>2</sub>PO<sub>4</sub> buffer (pH 7.1), 0.1 M NaNO<sub>3</sub>, and 10 mM Mg(NO<sub>3</sub>)<sub>2</sub>. The platinum compound (830  $\mu$ M) was then added and the solution was incubated at 37 °C for various time intervals. Pt(II)-bound DNA was then purified with Sephadex G-25 Medium size exclusion resin (GE Healthcare) on laboratory-prepared spin columns (BioRad) to remove unbound platinum. Purified samples were added (5.5  $\mu$ L) to 50% glycerol (9.5  $\mu$ L) and mixed. Samples were then loaded (10  $\mu$ L) on dPAGE (19:1 20% acrylamide in 8 M urea) and ran at 180 V. Gels were then stained with Methylene blue for 3 min and destained in diH<sub>2</sub>O for 30 min. Gels were then imaged using an Alpha Innotech UV Trans illuminator and quantified using ImageJ gel quantification methods. <sup>38</sup>

In Cell DNA-Pt(II) Binding Assays. Cell Treatment and Sample Preparation. A549 cells were seeded in a 150 mm culture dishes and incubated for at least 24 h or until at least 80% confluent, prior to treatment. Cell treatments were performed following the general treatment protocol. After incubation, the treatment media was aspirated, and cells were thoroughly washed three times with warm PBS (2 mL). Cells were harvested by trypsinization using 4 mL of TrypLE Express Enzyme (Thermo Fisher) and collected in 10 mL of DMEM in a 15 mL falcon tube. The cell suspension was then centrifuged (2000 rpm, 7 m), and the cell pellets were resuspended in 2 mL of cold PBS.

DNA Extraction and Quantification. DNA was extracted from cell pellets using a ZymoBIOMICS Quick-DNA Miniprep Kit. Clean DNA was extracted from collection columns into 1.5 mL Eppendorf tubes using diH<sub>2</sub>0 at a volume of 200  $\mu$ L per centrifuge column. Once collected the DNA concentration was taken for each sample using a Nanodrop (Thermofisher NanoDrop 1000). DNA was then dried at 37 °C under vacuum until all water had evaporated off.

Acid Digestion. For digestion, 100  $\mu$ L of concentrated nitric acid (69%, TraceSELECT, Fluka) was then added to each dry DNA sample and the sealed samples were heated at 65–70 °C on a heat block overnight. Digested samples were then cooled to RT and diluted with 900  $\mu$ L of diH<sub>2</sub>O to a final volume of 1 mL. Platinum quantification was performed by ICP-MS as described above.

**Molecular Modeling.** Energy minimization were performed as previously reported. <sup>8,10</sup> Briefly, compounds were optimized using density functional theory in Gaussian09. <sup>40</sup> Geometry optimizations were performed using a RMS force convergence criterion of 10–5 hartree. The electronic wave function was minimized using GGA functional PBE with the LANL2DZ basis set and compounds were rendered in Chimera X1.3 with 70% surface transparency. <sup>41,42</sup>

### ASSOCIATED CONTENT

# Supporting Information

The Supporting Information is available free of charge at https://pubs.acs.org/doi/10.1021/acschembio.2c00399.

In vitro DNA binding assays, additional cell images, and synthetic methods ( $\ensuremath{\text{PDF}}$ )

#### AUTHOR INFORMATION

## **Corresponding Author**

Victoria J. DeRose — Department of Chemistry and Biochemistry and Materials Science Institute, University of Oregon, Eugene, Oregon 97403, United States; oorcid.org/0000-0001-5761-671X; Email: derose@uoregon.edu

### **Authors**

- Hannah C. Pigg Department of Chemistry and Biochemistry, University of Oregon, Eugene, Oregon 97403, United States
- Matthew V. Yglesias Department of Chemistry and Biochemistry and Institute of Molecular Biology, University of Oregon, Eugene, Oregon 97403, United States; orcid.org/0000-0002-7511-8949
- Emily C. Sutton Department of Biology and Institute of Molecular Biology, University of Oregon, Eugene, Oregon 97403, United States
- Christine E. McDevitt Department of Chemistry and Biochemistry, University of Oregon, Eugene, Oregon 97403, United States
- Michael Shaw Department of Chemistry and Biochemistry, University of Oregon, Eugene, Oregon 97403, United States

Complete contact information is available at: https://pubs.acs.org/10.1021/acschembio.2c00399

#### Notes

The authors declare no competing financial interest.

# ACKNOWLEDGMENTS

This work was supported by the National Science Foundation [CHE2109255 to VJD and CHE2117614 for UO ICP-MS instrumentation] and the National Institutes of Health [T32 GM007759 to MYV and ECS]. Computations were performed with access to the University of Oregon HPC facility, Talapas. This work is also supported by the Department of Chemistry and Biochemistry, Department of Biology, Institute of Molecular Biology and the Material Science Institute at the University of Oregon.

### REFERENCES

- (1) Kelland, L. The Resurgence of Platinum-Based Cancer Chemotherapy. *Nat. Rev. Cancer* **2007**, *7* (8), 573–584.
- (2) Wexselblatt, E.; Yavin, E.; Gibson, D. Cellular Interactions of Platinum Drugs. *Inorg. Chim. Acta* **2012**, 393, 75–83.
- (3) Schoch, S.; Gajewski, S.; Rothfuß, J.; Hartwig, A.; Köberle, B. Comparative Study of the Mode of Action of Clinically Approved Platinum-Based Chemotherapeutics. *Int. J. Mol. Sci.* **2020**, *21* (18),
- (4) Bruno, P. M.; Liu, Y.; Park, G. Y.; Murai, J.; Koch, C. E.; Eisen, T. J.; Pritchard, J. R.; Pommier, Y.; Lippard, S. J.; Hemann, M. T. A Subset of Platinum-Containing Chemotherapeutic Agents Kills Cells by Inducing Ribosome Biogenesis Stress. *Nat. Med.* **2017**, 23 (4), 461–471.
- (5) Tsai, R. Y. L.; Pederson, T. Connecting the Nucleolus to the Cell Cycle and Human Disease. *FASEB J.* **2014**, 28 (8), 3290–3296.
- (6) Mars, J.-C.; Tremblay, M. G.; Valere, M.; Sibai, D. S.; Sabourin-Felix, M.; Lessard, F.; Moss, T. The Chemotherapeutic Agent CX-5461 Irreversibly Blocks RNA Polymerase I Initiation and Promoter Release to Cause Nucleolar Disruption, DNA Damage and Cell Inviability. NAR Cancer 2020, 2 (4), 1–15.
- (7) Jacobs, R. Q.; Huffines, A. K.; Laiho, M.; Schneider, D. A. The Small-Molecule BMH-21 Directly Inhibits Transcription Elongation

- and DNA Occupancy of RNA Polymerase I in Vivo and in Vitro. J. Biol. Chem. 2022, 298 (1), 101450.
- (8) Sutton, E. C.; McDevitt, C. E.; Prochnau, J. Y.; Yglesias, M. V.; Mroz, A. M.; Yang, M. C.; Cunningham, R. M.; Hendon, C. H.; DeRose, V. J. Nucleolar Stress Induction by Oxaliplatin and Derivatives. J. Am. Chem. Soc. 2019, 141 (46), 18411–18415.
- (9) Sutton, E. C.; DeRose, V. J. Early Nucleolar Responses Differentiate Mechanisms of Cell Death Induced by Oxaliplatin and Cisplatin. *J. Biiol. Chem.* **2021**, *296*, 100633.
- (10) McDevitt, C. E.; Yglesias, M. V.; Mroz, A. M.; Sutton, E. C.; Yang, M. C.; Hendon, C. H.; DeRose, V. J. Monofunctional Platinum(II) Compounds and Nucleolar Stress: Is Phenanthriplatin Unique? *J. Biol. Inorg. Chem.* **2019**, *24* (6), 899–908.
- (11) McDevitt, C. E.; Guerrero, A. S.; Smith, H. M.; DeRose, V. J. Influence of Ring Modifications on Nucleolar Stress by Oxaliplatin-like Compounds. *ChemBioChem* **2022**, e202200130.
- (12) Peterson, E. J.; Menon, V. R.; Gatti, L.; Kipping, R.; Dewasinghe, D.; Perego, P.; Povirk, L. F.; Farrell, N. P. Nucleolar Targeting by Platinum: P53-Independent Apoptosis Follows RRNA Inhibition, Cell-Cycle Arrest, and DNA Compaction. *Mol. Pharmaceutics* **2015**, *12* (1), 287–297.
- (13) Rubbi, C. P.; Milner, J. Disruption of the Nucleolus Mediates Stabilization of P53 in Response to DNA Damage and Other Stresses. *EMBO J.* **2003**, 22 (22), 6068–6077.
- (14) Yang, K.; Wang, M.; Zhao, Y.; Sun, X.; Yang, Y.; Li, X.; Zhou, A.; Chu, H.; Zhou, H.; Xu, J.; Wu, M.; Yang, J.; Yi, J. A Redox Mechanism Underlying Nucleolar Stress Sensing by Nucleophosmin. *Nat. Commun.* **2016**, *7*, 13599.
- (15) Yung, B. Y.; Busch, R. K.; Busch, H.; Mauger, A. B.; Chan, P. K. Effects of Actinomycin D Analogs on Nucleolar Phosphoprotein B23 (37,000 Da/PI 5.1). *Biochem. Pharmacol.* **1985**, 34 (22), 4059–4063.
- (16) Ahmad, S. Kinetic Aspects of Platinum Anticancer Agents. *Polyhedron* **2017**, *138*, 109–124.
- (17) Burger, K.; Mühl, B.; Harasim, T.; Rohrmoser, M.; Malamoussi, A.; Orban, M.; Kellner, M.; Gruber-Eber, A.; Kremmer, E.; Hölzel, M.; Eick, D. Chemotherapeutic Drugs Inhibit Ribosome Biogenesis at Various Levels. J. Biol. Chem. 2010, 285 (16), 12416–12425.
- (18) Hall, M. D.; Okabe, M.; Shen, D.-W.; Liang, X.-J.; Gottesman, M. M. The Role of Cellular Accumulation in Determining Sensitivity to Platinum-Based Chemotherapy. *Annu. Rev. Pharmacol. Toxicol.* **2008**, *48* (1), 495–535.
- (19) Levina, A.; Crans, D. C.; Lay, P. A. Speciation of Metal Drugs, Supplements and Toxins in Media and Bodily Fluids Controls in Vitro Activities. *Coord. Chem. Rev.* **2017**, *352*, 473–498.
- (20) Ghezzi, A.; Aceto, M.; Cassino, C.; Gabano, E.; Osella, D. Uptake of Antitumor Platinum(II)-Complexes by Cancer Cells, Assayed by Inductively Coupled Plasma Mass Spectrometry (ICP-MS). J. Inorg. Biochem. 2004, 98 (1), 73–78.
- (21) Hermann, G.; Heffeter, P.; Falta, T.; Berger, W.; Hann, S.; Koellensperger, G. In Vitro Studies on Cisplatin Focusing on Kinetic Aspects of Intracellular Chemistry by LC-ICP-MS. *Metallomics* **2013**, 5 (6), 636.
- (22) Yamada, K.; Kato, N.; Takagi, A.; Koi, M.; Hemmi, H. One-Milliliter Wet-Digestion for Inductively Coupled Plasma Mass Spectrometry (ICP-MS): Determination of Platinum-DNA Adducts in Cells Treated with Platinum(II) Complexes. *Anal. Bioanal. Chem.* **2005**, 382 (7), 1702–1707.
- (23) Bednarski, P. J.; Trümbach, B. Use of Reversed-Phase HPLC for Determination of the Hydrolysis Rate Constants of Dichloro(1,2-Diarylethylenediamine)Platinum(II) Complexes. *Transition. Met. Chem.* **1994**, *19* (5), 513–517.
- (24) Hah, S. S.; Sumbad, R. A.; de Vere White, R. W.; Turteltaub, K. W.; Henderson, P. T. Characterization of Oxaliplatin–DNA Adduct Formation in DNA and Differentiation of Cancer Cell Drug Sensitivity at Microdose Concentrations. *Chem. Res. Toxicol.* **2007**, 20 (12), 1745–1751.
- (25) Jamieson, E. R. A. Potential Cellular Targets for Cisplatin. Chem. Rev. 1999, 99, 2467–2498.

- (26) Chaney, S. G.; Campbell, S. L.; Bassett, E.; Wu, Y. Recognition and Processing of Cisplatin- and Oxaliplatin-DNA Adducts. *Crit. Rev. in Oncol. Hematol.* **2005**, 53 (1), 3–11.
- (27) Woynarowski, J. M.; Faivre, S.; Herzig, M. C.; Arnett, B.; Chapman, W. G.; Trevino, A. V.; Raymond, E.; Chaney, S. G.; Vaisman, A.; Varchenko, M.; Juniewicz, P. E. Oxaliplatin-Induced Damage of Cellular DNA. *Mol. Pharmacol.* **2000**, 58 (5), 920–927.
- (28) Johnson, B. W.; Burgess, M. W.; Murray, V.; Aldrich-Wright, J. R.; Temple, M. D. The Interactions of Novel Mononuclear Platinum-Based Complexes with DNA. *BMC Cancer* **2018**, *18* (1), 1284.
- (29) Alian, O. M.; Azmi, A. S.; Mohammad, R. M. Network Insights on Oxaliplatin Anti-Cancer Mechanisms. *Clin. Trans. Med.* **2012**, *1* (1), 26.
- (30) Raymond, E.; Faivre, S.; Chaney, S.; Woynarowski, J.; Cvitkovic, E. Cellular and Molecular Pharmacology of Oxaliplatin1. *Mol. Cancer Ther.* **2002**, *1* (3), 227–235.
- (31) Saris, C. P.; van de Vaart, PJ. M.; Rietbroek, R. C.; Bloramaert, F. A. In Vitro Formation of DNA Adducts by Cisplatin, Lobaplatin and Oxaliplatin in Calf Thymus DNA in Solution and in Cultured Human Cells. *Carcinogenesis* **1996**, *17* (12), 2763–2769.
- (32) Zhang, H.-Y.; Liu, Y.-R.; Ji, C.; Li, W.; Dou, S.-X.; Xie, P.; Wang, W.-C.; Zhang, L.-Y.; Wang, P.-Y. Oxaliplatin and Its Enantiomer Induce Different Condensation Dynamics of Single DNA Molecules. *PLoS One* **2013**, *8* (8), e71556.
- (33) Schoch, S.; Gajewski, S.; Rothfuß, J.; Hartwig, A.; Köberle, B. Comparative Study of the Mode of Action of Clinically Approved Platinum-Based Chemotherapeutics. *Int. J. of Mol. Sci.* **2020**, *21* (18), 6928.
- (34) Rose, P. K.; Watkins, N. H.; Yao, X.; Zhang, S.; Mancera-Ortiz, I. Y.; Sloop, J. T.; Donati, G. L.; Day, C. S.; Bierbach, U. Effect of the Nonleaving Groups on the Cellular Uptake and Cytotoxicity of Platinum-Acridine Anticancer Agents. *Inorganic Chim. Acta.* **2019**, 492, 150–155.
- (35) Suchánková, T.; Kubíček, K.; Kašpárková, J.; Brabec, V.; Kozelka, J. Platinum–DNA Interstrand Crosslinks: Molecular Determinants of Bending and Unwinding of the Double Helix. *J. Inorg. Biochem.* **2012**, *108*, 69–79.
- (36) Desoize, B.; Madoulet, C. Particular Aspects of Platinum Compounds Used at Present in Cancer Treatment. *Crit. Rev. Oncol. Hematol.* **2002**, 42 (3), 317–325.
- (37) Vekris, A.; Meynard, D.; Haaz, M.-C.; Bayssas, M.; Bonnet, J.; Robert, J. Molecular Determinants of the Cytotoxicity of Platinum Compounds: The Contribution of in Silico Research. *Cancer Res.* **2004**, *64* (1), 356–362.
- (38) Rueden, C. T.; Schindelin, J.; Hiner, M. C.; DeZonia, B. E.; Walter, A. E.; Arena, E. T.; Eliceiri, K. W. ImageJ2: ImageJ for the next generation of scientific image data. *BMC Bioinform.* **2017**, *18*, 529.
- (39) van der Walt, S.; Schönberger, J. L.; Nunez-Iglesias, J.; Boulogne, F.; Warner, J. D.; Yager, J.; Gouillart, E.; Yu, T. and the scikit-image contributors. *scikit-image: Image processing in Python*; PeerJ 2:e453, 2014.
- (40) Frisch, M. J.; Trucks, G. W.; Schlegel, H. B.; Scuseria, G. E.; Robb, M. A.; Cheeseman, J. R.; Scalmani, G.; Barone, V.; Petersson, G. A.; Nakatsuji, H. et al. *Gaussian09*; Gaussian, Inc., Wallingford, CT, 2016.
- (41) Perdew, J. P.; Burke, K.; Ernzerhof, M. Generalized Gradient Approximation Made Simple. *Phys. Rev. Lett.* **1996**, *77*, 3865–3868.
- (42) Perdew, J. P.; Burke, K.; Ernzerhof, M. Errata: Generalized Gradient Approximation Made Simple. *Phys. Rev. Lett.* **1997**, 78, 1396.